Hindawi Publishing Corporation
Journal of Nanomaterials
Volume 2016, Article ID 3038790, 9 pages
http://dx.doi.org/10.1155/2016/3038790

Research Article

Computational Modeling of the Effect of Sulci during Tumor Growth and Cerebral Edema

Dan Peng,[1] Zhiheng Zhou,[2] Yin Liu,[2] Tianfu Guo,[3] Ying Li,[4] and Shan Tang[2]

[1]*Department of Neurology, Chongqing General Hospital, Yuzhong, Chongqing 400000, China*
[2]*School of Aerospace Engineering, Chongqing University, Shapingba, Chongqing 400017, China*
[3]*Institute of High Performance Computing, A*STAR, Singapore 138632*
[4]*Department of Mechanical Engineering, Institute of Materials Science, University of Connecticut, Storrs, CT 06269, USA*

Correspondence should be addressed to Ying Li; yingli@engr.uconn.edu and Shan Tang; shan_tang_0917@163.com

Received 30 December 2015; Accepted 5 May 2016

Academic Editor: Stefano Bellucci

This paper aims at studying the effect of sulci structures during tumor growth and cerebral edema in brain tissues. Motivated by the Intracranial Cerebral Pressure (ICP) monitoring during the brain surgery, a computational model has been created to study macroscopic behaviors of brain tissues with local volume expansion introduced by the tumor growth and cerebral edema. To consider the extra-large deformation during the tumor growth, a nonlinear finite element method has been adopted. Numerical simulation results reveal that sulci structures play significant roles in macroscopic volume expansion and maximum stress of brain tissues. Without considering the sulci structures, predictions on the ICP will be dramatically different from those including sulci structure. Therefore, it is strongly suggested that the sulci structure should be included in future studies on the brain modeling for investigating the space-occupying lesions.

1. Introduction

The revised Monro-Kellie hypothesis describes that the total volume of brain tissues, intracranial blood, and cerebrospinal fluid is constant in a skull [1, 2]. Therefore, increasing the volume fraction of one component will reduce the volume of the remaining one or two. Brain tumors can expand their volumes through proliferation within brain tissues [3]. However, the brain tissue's mechanically reserved room, that is, the interstitial space, cerebrospinal fluid filled ventricles, and vascular systems, can only temporarily compensate through the fluid flow. Once the critical point of decompensation is reached, a minor increment of brain tissue's volume can cause a massive, life-threatening development of Intracranial Cerebral Pressure (ICP) [4]. The traumatic brain injury will induce the cerebral edema in the brain tissues. Due to the diffusion of the blood into places with cerebral edema, the brain tissues grow and expand, resulting in a rise in ICP [5]. The normal brain and its related various pathological changes, which can cause the growth and expansion of brain tissues, are shown in Figure 1. Decompressive craniectomy is the final phase in the graded scheme of critical care management of refractory raised ICP [6, 7]. Although the decompressive craniectomy can reduce the ICP, the related process may further introduce the transcalvarial herniation [8], coming from the expansion of brain tissues with lower outer pressure (i.e., from the cerebrospinal fluid pressure to air pressure).

With advancements in computational methods [9, 10], finite element analysis (FEA) has been used to investigate the brain under pathological changes as done by Goriely et al. [11]; Budday et al. [12]; Goriely et al. [13]; and Budday et al. [14, 15]. For example, Mohamed and Davatzikos [16] studied the mass effect of brain tumors through 3D FEA modeling. The contraction of brain tissues due to the resection of tumors has been investigated in detail. Through FEA modeling, the effects of a number of parameters, such as tumor size, location, and peritumor edema extent, can be uncovered. Gao and Ang [8] explored the brain deformation and ICP changes with unilateral frontoparietal-temporal and bifrontal decompressive craniectomy through FEA. The obtained simulation results can be used to guide the optimal

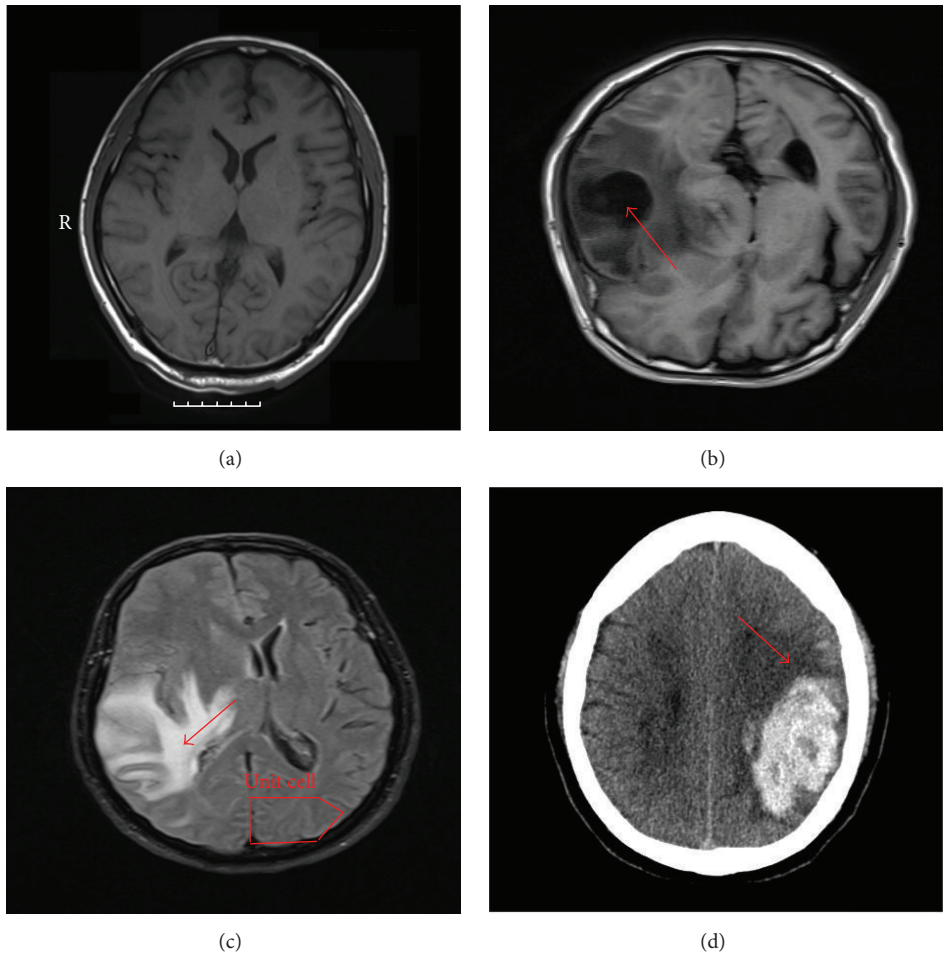

Figure 1: Normal brain and its related various pathological changes: (a) normal brain; (b) with tumor; (c) with cerebral edema; and (d) with cerebral hemorrhage. The arrows indicate the locations at which the tumor growth, cerebral edema, and cerebral hemorrhage take place. These medical images are taken from three patients at Chongqing General Hospital.

conduct of decompressive surgery with minimum impact on transcalvarial brain herniation. Sulcal deformation in normal pressure hydrocephalus (NPH) has been studied by Kim et al. [17].

It is well-known that the surface morphology of brain tissues is usually related to the intelligence and neurological dysfunction of human beings [11, 18]. Therefore, the formation of sulci structures in brain has attracted a lot of attention recently. Budday et al. [19] and Razavi et al. [20, 21] built an analytic model and established a computational model, respectively, using the continuum mechanics theory to explain the formation of surface folds on brain tissues. Their models are capable of predicting the formation of complex surface morphologies with sulci structures, demonstrating the important role of mechanics in the development of brains [13, 14, 19]. Through the variations in cortical and subcortical thickness, stiffness, or growth, different patterns can be formed on the brain surface [22]. The formation of sulci structures is found to be related to the surface instability of soft matters, such as wrinkles on nanofibers [23, 24], bilayered elastomers [25], and core-shell structures [26, 27]. Though significant progress has been made in recent years with respect to the modeling of morphological evolution of developing brains, there are still many remaining open questions.

In present study, we are trying to explore the existing sulci structures during the cerebral edema and tumor growth in the brain tissue, rather than studying the formation mechanisms of the sulci structure. In a previous study [17], two FEA models have been developed: an anatomical brain geometric (ABG) model and a conventional simplified brain geometric (SBG) model. However, most studies use the SBG model, ignoring the details of sulci geometry at the edges of brain tissues. Recent studies suggest that structural characteristics of the sulci structure could play an important role when the brain is under mechanical stress [28, 29]. For instance, Kim et al. [17] investigated the degree of tissue distortion in NPH with and without sulci. Their results uncover that the SBG model can significantly underestimate the pathologic changes during the development of NPH. In this work, we focus on the structural evolution of the sulci during the tumor growth and cerebral edema through FEA. The sulci effects on ICP

and stress distribution in the brain tissue are also investigated in detail. The obtained simulation results are expected to shed light on the realistic modeling of the tumor growth and cerebral edema, eventually providing useful guidelines for the surgical procedure.

2. Model and Methods

In this study, we use the hydrogel model to describe the mechanical behaviors of brain tissues, which is different from the previous researchers [16, 17]. In these previous studies, the Neo-Hookean model with thermal volume ratio has been widely used. However, the fluid flow within the brain tissue is often ignored. To consider the effects of the blood flow in brain tissues (in particular, the cerebral edema is caused by the flow-in water), the hydrogel model, developed by Hong et al. [30] and Zhang et al. [31], is used to study the brain edema. Although tumor growth is not related to fluid flow, the model still can describe the volume expansion caused by cell growth. Such a model has attracted a lot of attention for polymeric hydrogels [32, 33]. It has been demonstrated that the model with a nonlinear field theory can be used to analyze large deformations in hydrogels [30, 31]. In the theoretical formulation [30], the free energy density of the hydrogel takes the dry, solvent-free network as the reference state. In reality, gel-like materials, such as brain tissues, contain a large amount of solvent molecules and are never dry. Moreover, the cerebral fluids and blood can flow within brain tissues. In this case, we take the swollen state, rather than the dry state, as a reference state and denote it as the initial configuration. The theoretical model developed by Wong et al. [34, 35] and Zhang et al. [31] is adopted. The main equations in Wong et al. [34] are recapitulated in the following. The interested reader can refer to their original work.

Under the large deformation assumption, the point $\mathbf{X}$ under the initial configuration moves to $\mathbf{x}$ under the current configuration. Then, the deformation gradient can be defined as

$$\mathbf{F} = \frac{\partial \mathbf{x}}{\partial \mathbf{X}}. \tag{1}$$

Denoting ϕ_0 as the initial polymer volume fraction, its free energy density W can be defined as

$$\begin{aligned}\frac{W}{KT/v} = {} & \frac{N_v}{2}\phi_0^{1/3}\left(I_1 - 3\right) - 2\phi_0 \ln J \\ & + \left(J - \phi_0\right)\ln\left(1 - \frac{\phi_0}{J}\right) \\ & - \left(1 - \phi_0\right)\ln\left(1 - \phi_0\right) + \chi\phi_0^2\left(1 - \frac{\phi_0}{J}\right) \\ & - \frac{\mu_0}{KT}\left(J - 1\right) - \frac{\delta\mu}{KT}\left(J - \phi_0\right),\end{aligned} \tag{2}$$

where the first invariant $I_1 = F_{iK}F_{iK}$ and Jacobian $J = \det(\mathbf{F})$. Here N is the number of chains per volume, v is the volume per solvent molecule, and χ is Flory-Huggins parameter, characterizing the enthalpy of mixing of polymer and solvent molecules. K is the Boltzmann constant and T is the temperature. Note that $N_v = Nv$. Since we take the swollen state as the reference configuration, it will introduce the chemical potential at this state μ_0

$$\frac{\mu_0}{KT} = N_v\phi_0^{1/3} + \chi\phi_0^2 + \left(1 - N_v\right)\phi_0 + \ln\left(1 - \phi_0\right), \tag{3}$$

where $\delta\mu/KT$ is the variation of the chemical potential with respect to the reference configuration. The initial (undeformed) state is denoted by $\delta\mu/\mu_0 = 0$. Deswelling of the constrained gel is represented by $\delta\mu/\mu_0 > 0$, while $\delta\mu/\mu_0 < 0$ for swelling ones. In this work, we set $\delta\mu/\mu_0 < 0$ to describe the swelling induced by the tumor growth and cerebral edema, as the blood flows into these regions. Unless otherwise stated, the material parameters used in this study are as follows:

$$\begin{aligned} N_v &= 1.0 \times 10^{-3}, \\ \chi &= 0.1, \\ \phi_0 &= 0.1. \end{aligned} \tag{4}$$

Note that these parameters are chosen to study the sulci structure effect on tumor growth and cerebral edema. Future experimental studies are required to identify more accurate material parameters. We stress again that further experimental study needs to be carried out to testify if hydrogel model is appropriate for brain tissues during brain edema and tumor growth. The present work is a preliminary study and can only shed some light on how expansion can influence the mechanical behaviors of brains.

All the FEA simulations are performed under the 2D axisymmetric conditions by using the commercial finite element software ABAQUS [36]. Although the full 3D modeling is possible and could be closer to the real situation, it will involve more parameters to be determined. To understand the important effect of sulci structure, this preliminary analysis only considers the 2D case. A representative unit cell, as depicted in Figures 1 and 2, is used to represent a simplified brain model. Here the representative unit cell (cf. Figure 2(a)) can be considered as a part from the real brain images shown in Figure 1(c) (red polygon). Since the depth of the sulci structure could vary at different locations, we consider two different initial depths of sulci structure in this study: $h_0/H = 0.05$ and 0.3 (the height of the unit cell is H; see Figure 2). The depth of sulci can be measured in CT or MRT images of brain. Another unit cell without sulci structure is also considered to explore the sulci effect (cf. Figure 2(b)). The tumor growth and cerebral edema at different locations are considered, marked by shaded area, such as A_1 to A_9 and B_1 to B_9 in Figure 2. The unit cell has been discretized by about 16,000 four-node quadrilateral CAXH4 elements (axisymmetric elements) in ABAQUS. The corresponding boundary conditions are also given in Figures 2(a) and 2(b). Implicit time integration is performed for the nonlinear geometric analysis. To provide a direct insight into the parameter $\delta\mu$ effect, we perform another simulation over a single element with the left and bottom edges fixed along x and y directions (cf. Figure 2(c)), respectively. Then,

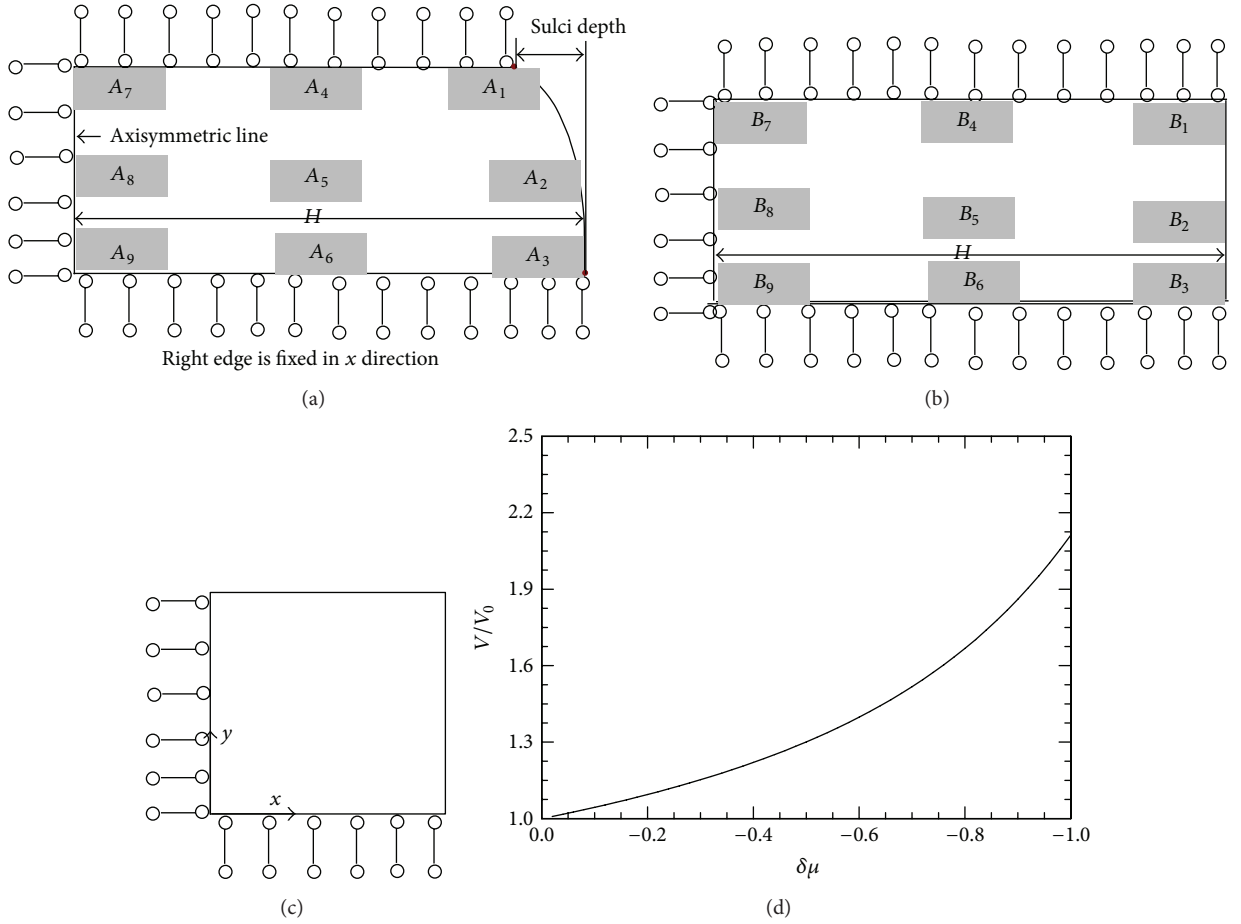

FIGURE 2: Simplified unit cell models: (a) with sulci structure; (b) without sulci structure; (c) a single element model to demonstrate $\delta\mu$ effect; (d) volume expansion versus $\delta\mu$ for a single element. Boundary conditions are shown and the locations where the local tumor growth/cerebral edema occurs are marked by gray areas.

the value of $\delta\mu$ is increased to compute the volume at the current configuration. The corresponding result is given in Figure 2(d). It can be seen that the volume expands with the increment of $\delta\mu$. At $\delta\mu/\mu_0 = -1$, the volume expansion of the element is about 100%.

3. Results and Discussion

We firstly investigate the difference in total volume expansion with and without sulci structure. Figures 3(a) and 3(b) demonstrate the ratio of current volume to initial volume as a function of $\delta\mu$ for $h_0/H = 0.3$ and 0.05, respectively. All the results are compared with the same local volume expansion at locations A_4, A_5, A_6 with sulci and corresponding locations B_4, B_5, B_6 without sulci. From these results, it is clearly shown that the local volume expansion of the brain tissue with sulci structure (A_4, A_5, A_6) is faster than that without sulci structure (B_4, B_5, B_6). When the thickness of the sulci is enlarged from 0.05 to 0.3, this effect is more pronounced (cf. Figure 3). It also indicates that larger initial depth of sulci structure can result in larger volume expansion during the tumor growth and cerebral edema. As we know, the depth of the sulci structure varies along the surface of brain tissue (cf. Figure 1). If the tumor growth/cerebral edema occurs at a place with different sulci depths, the resulting volume expansions will be different. During the surgery, this effect should be taken into consideration. Once the point of decompensation is reached, a minor increase in volume could trigger a massive, life-threatening increase in ICP [5].

Then, we investigate the total volume expansion induced by the same local volume expansion at different places during the tumor growth and cerebral edema. The obtained results are shown in Figure 4. The obtained curves for the ratio of current volume to initial volume are delineated into three different regions. For the locations closer to sulci structure (A_1, A_2, A_3), the volume expansion is larger and the local volumes increase much faster with increasing $\delta\mu$. However, for the locations far away from the sulci structure (A_7, A_8, A_9), the volume expansion is much smaller and the increment of local volumes is slower. These findings are very important for the clinical surgery. A patient with traumatic brain injury usually needs a Computed Tomography (CT) scan before the surgery. Then, the place with local cerebral edema can be found. If the location is far away from the sulci,

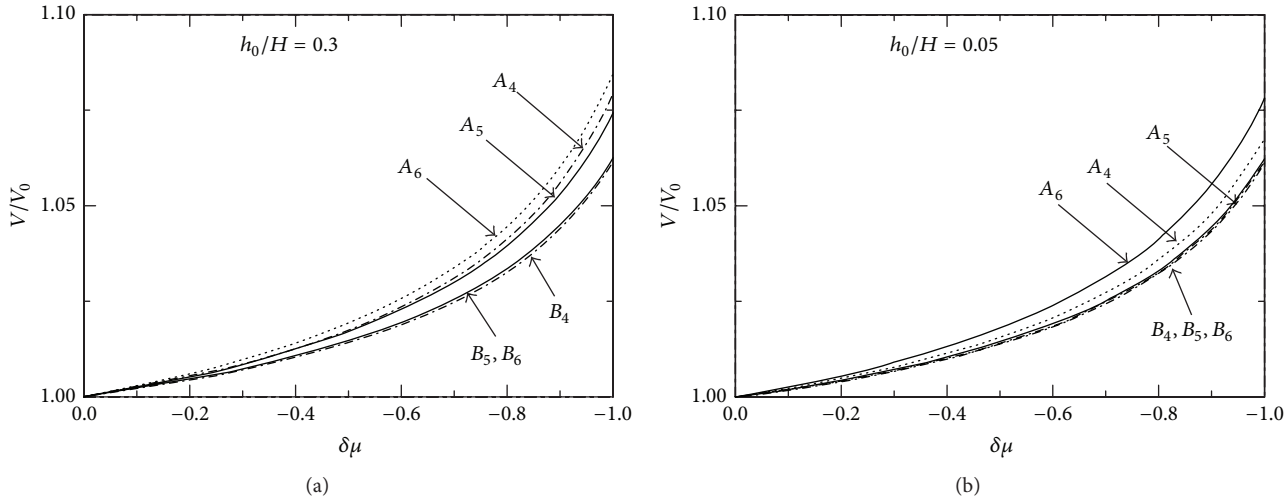

FIGURE 3: Ratio of the current volume to initial volume as a function of $\delta\mu$ (local tumor growth/cerebral edema) with (a) $h_0/H = 0.3$ and (b) $h_0/H = 0.05$.

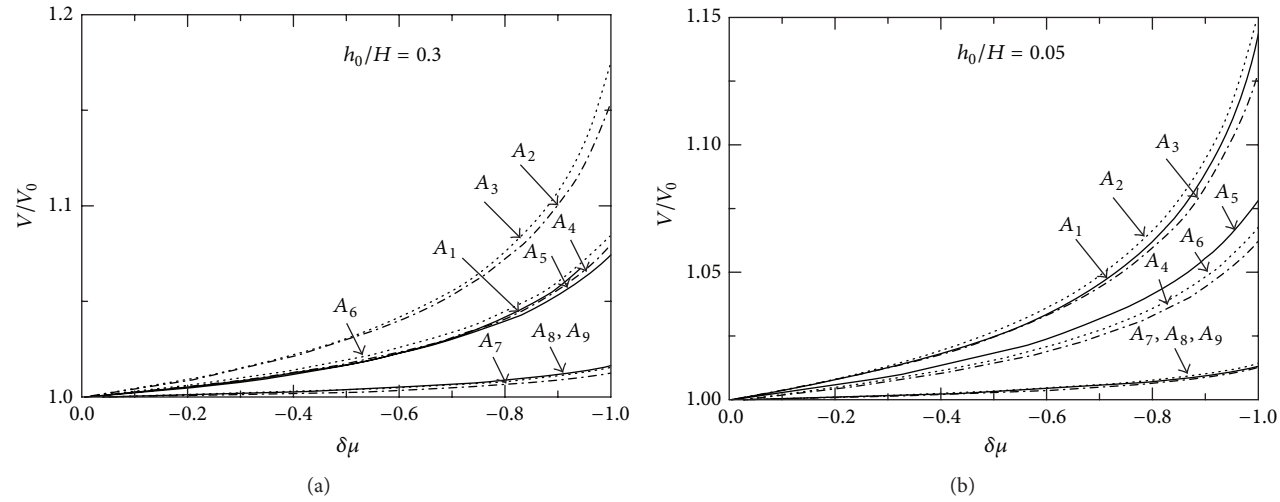

FIGURE 4: Ratio of the current volume to initial volume as a function of $\delta\mu$ (local tumor growth/cerebral edema) at different locations: (a) $h_0/H = 0.3$ and (b) $h_0/H = 0.05$.

the ICP is less severe than the place close to the sulci structure. Thus, the doctors may find other ways to handle the situation.

The deformation of sulci structure during the tumor growth/cerebral edema is also measured and given in Figure 5, as a function of $\delta\mu$. Here the sulci depth is measured as the distance in horizontal direction between the maximum x point and the valley point of sulci (cf. Figure 2). When the location of tumor growth/cerebral edema is close to sulci (A_1, A_2, A_3), the measured sulci depth increases with decreasing $\delta\mu$, while for these locations far away from sulci, with $\delta\mu$ (local expansion) decreasing, the sulci depth will also be reduced. In most of the clinical situations, the tumor growth/cerebral edema often happens at the locations far away from the sulci. Therefore, it is usually stated contextually that the depth of sulci will decrease during the tumor growth/cerebral edema [37]. According to our simulation results, this may not be true for all the cases. The depth of sulci depends on both the initial depth of sulci and the location of tumor growth/cerebral edema that takes place.

Compared to other methods, the advantage of FEA is that it cannot only capture the deformation of brain tissue, but also can predict the stress distributions. The local pressure and von Mises stress are important parameters to evaluate the extent of damage in brain tissues and can be adopted by doctors for their surgery. If the pressure is very high for some locations, the blood vessel may be compressed, resulting in the blood clot or vessel breaking. This situation could be very dangerous. In the following part, we will examine the stress and pressure distributions during the tumor growth/cerebral edema.

The local pressure distributions with and without sulci are given in Figure 6. The initial depth of the sulci is taken to be $h_0/H = 0.3$. The results are compared with the same local volume expansion induced by the tumor growth/cerebral

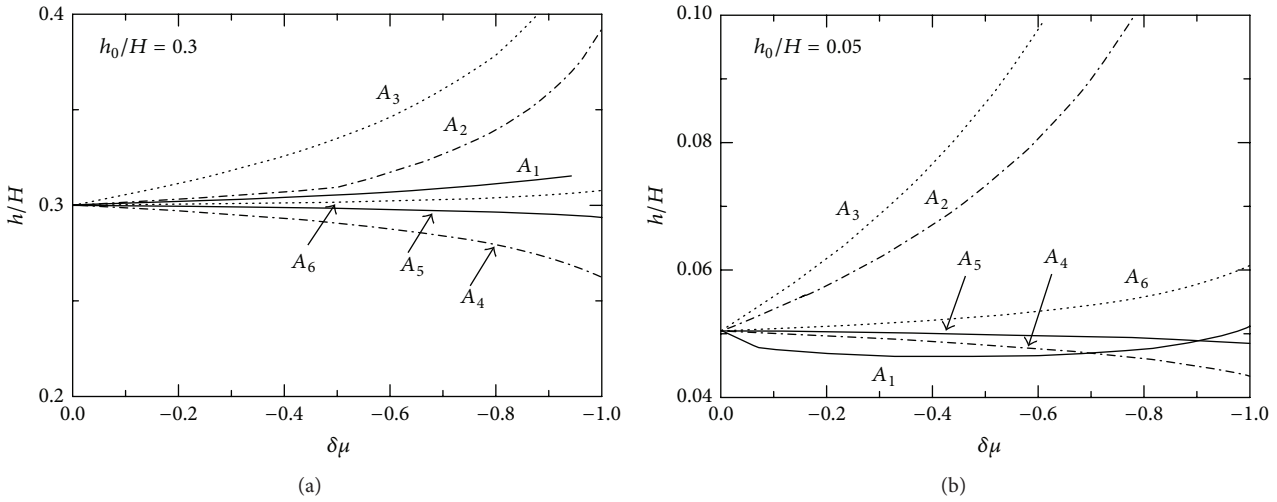

FIGURE 5: Depth of the sulci structure as a function of $\delta\mu$. The definition of the sulci depth is given in Figure 2.

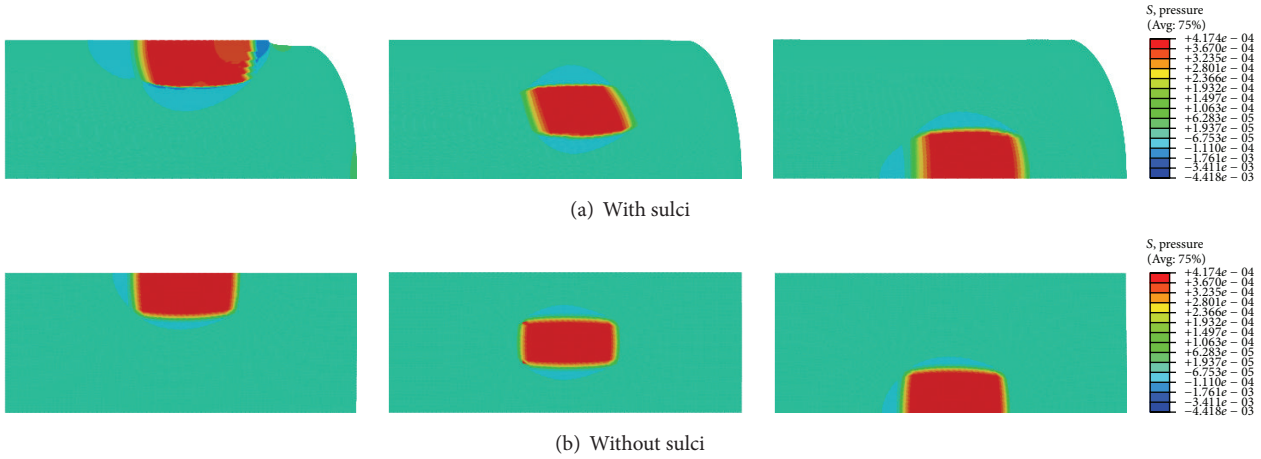

FIGURE 6: Comparison of pressure distribution between unit cell models with and without sulci structures. The initial depth of the sulci is taken to be $h_0/H = 0.3$. The stress is normalized by NKT.

edema (A_4, A_5, A_6 and corresponding B_4, B_5, B_6). It can be seen that the highest pressure comes from the place with tumor growth/cerebral edema. This situation is consistent with our intuition. From Figure 6, the negative pressure region around the area with highest pressure is much larger for the tissue with sulci, compared to that without sulci. If the tumor growth/cerebral edema takes place at A_4, there exists a high pressure region at the valley of sulci, which may influence the surgery.

The von Mises stress distributions with and without sulci are presented in Figure 7. The initial depth of the sulci is set to be $h_0/H = 0.3$. The results are compared with the same local volume expansion induced by the tumor growth/cerebral edema (A_4, A_5, A_6 and correspondingly B_4, B_5, B_6). From Figure 7, the von Mises stress for locations A_5 and A_6, where the local volume expansion takes place, is nearly the same, regardless of whether the sulci structure is considered or not. However, comparing the results for locations A_4 and B_4, the von Mises stress is much higher, especially at the valley of sulci, when the sulci is considered.

Finally, we generate a simple brain model based on the images used in Kim et al. [17]. Then, the tumor growth/cerebral edema is considered to take place as illustrated in Figure 2(b). Here, only half of a brain is shown because we assume the axisymmetric geometry of the brain. Figure 8 plots the von Mises stress and pressure distributions with and without sulci. Again, we find that the brain with sulci structure demonstrates larger von Mises stress at the same location. This observation is consistent with our above unit cell analysis (cf. Figures 6 and 7). Moreover, with the sulci structure, the large stress value can be transmitted to further regions, as depicted in Figure 8.

The total volume of the brain as a function of $\delta\mu$ is given in Figure 9. The total volume is found to increase much faster for that with sulci structure. Again, this finding is consistent with our above unit cell analysis (cf. Figure 3).

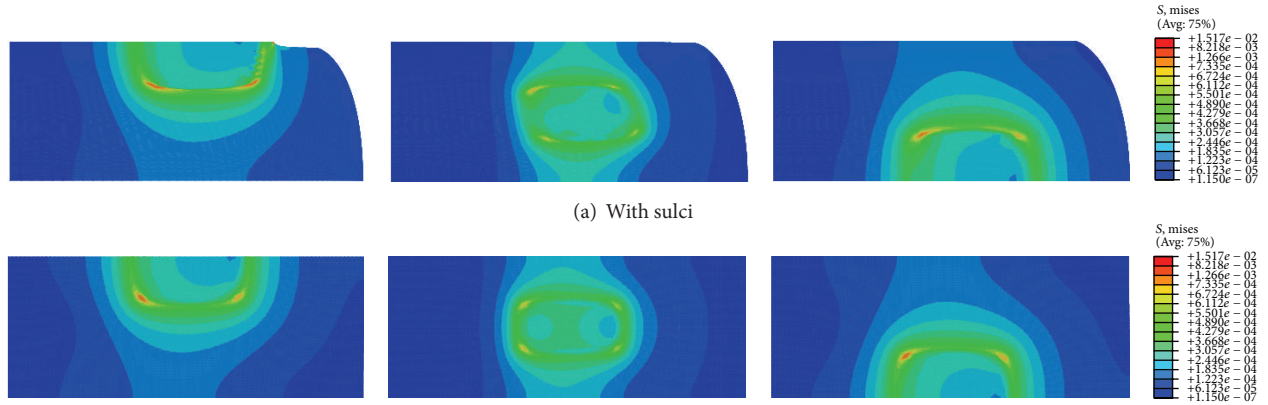

(a) With sulci

(b) Without sulci

Figure 7: Comparison of von Mises stress distribution between unit cell models with and without sulci structures. The initial depth of the sulci is taken to be $h_0/H = 0.3$. The stress is normalized by NKT.

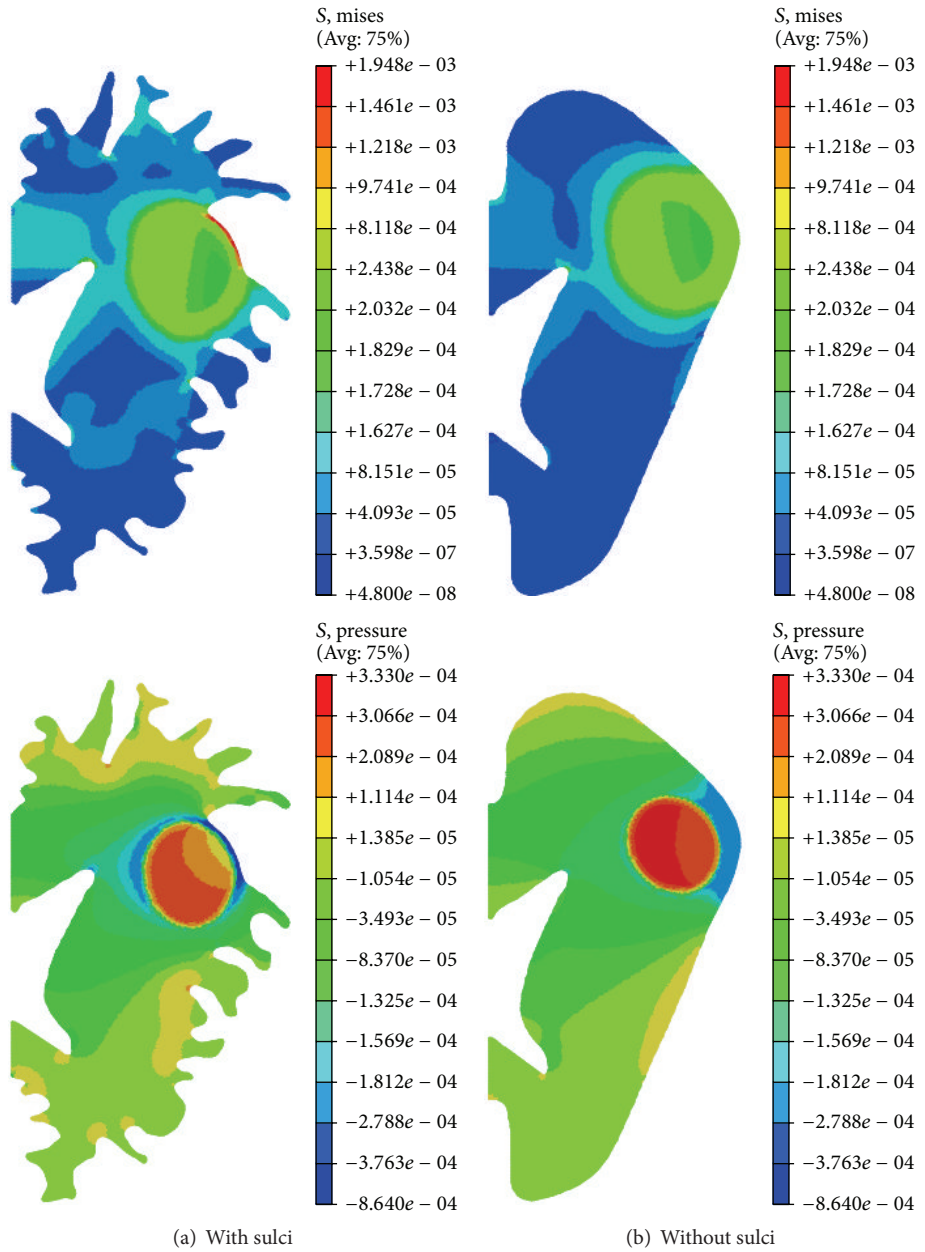

(a) With sulci

(b) Without sulci

Figure 8: Comparison of von Mises stress and pressure distributions between brain models with and without sulci structures. The stress is normalized by NKT.

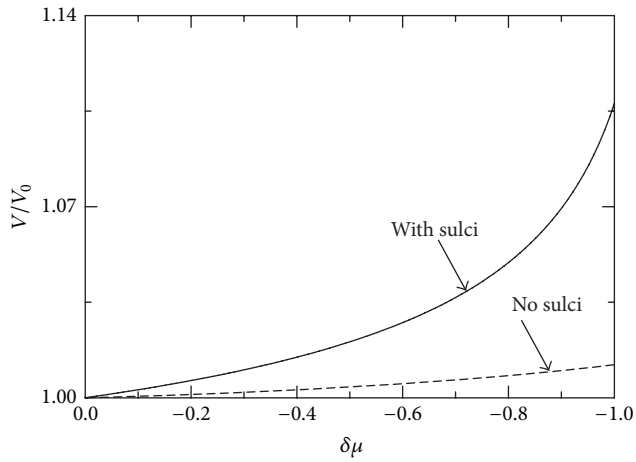

Figure 9: Ratio of the current volume to initial volume as a function of $\delta\mu$ (local tumor growth/cerebral edema) for the simplified brain model.

Although the unit cell model is simple, it does provide the fundamental insights into the local volume expansion, pressure, and stress distributions of the brain tissue during tumor growth/cerebral edema. Finally, we should emphasize the important role played by the sulci structures on ICP, as they can influence the local volume expansion dramatically.

4. Conclusion

In this work, a preliminary study on the effects of sulci structure during tumor growth/cerebral edema has been carried out. Through simplified unit cell and brain models, we find that the sulci structure plays an important role in the local volume expansion, pressure, and von Mises stress distributions in brain tissues. If the sulci structure is ignored, the local volume change, pressure, and von Mises stress will be significantly underestimated, resulting in lower prediction on ICP. Evidently, the consideration of the sulci structure is necessary for a more accurate representation.

Finally, we also need to point out certain limitations of present study. Due to the complexity of the brain and brain tissue, we only consider the simplified unit cell and brain models to study the sulci effect. Such a simplified model cannot capture the real pathological changes of a brain with tumor growth/cerebral edema. In the future study, a full 3D model of the whole brain should be used, which can give more accurate predictions on the volume expansion, pressure, and stress distributions. In addition, we adopt the hydrogel model to describe the mechanical behaviors of brain tissues. Though such a model can easily simulate the growth of brain tissue related to the tumor growth/cerebral edema, we did not distinguish the difference of white matter and gray matter in the brain. The difference between them may lead to a response, different from our current predictions. Although we believe that the trends given by the present model should still hold, future studies will be explored to consider the difference between the white and gray matters, as well as more accurate material parameters calibrated through experiments.

Competing Interests

The authors declare that they have no competing interests.

Acknowledgments

Dan Peng appreciates the support of NHFPC of Chongqing (Project no. 2015MSXM075). Shan Tang thanks "Young Thousand Talented Program," NSF of Chongqing (Project no. 0211002431039:cstc2013jcyjA50010), and NSF of China (Project no. 11472065). Ying Li acknowledges support from the Department of Mechanical Engineering at University of Connecticut.

References

[1] B. Mokri, "The monro-kellie hypothesis: applications in CSF volume depletion," *Neurology*, vol. 56, no. 12, pp. 1746–1748, 2001.

[2] L. H. Weed, "Some limitations of the monro-kellie hypothesis," *Archives of Surgery*, vol. 18, no. 4, pp. 1049–1068, 1929.

[3] S. K. Singh, I. D. Clarke, M. Terasaki et al., "Identification of a cancer stem cell in human brain tumors," *Cancer Research*, vol. 63, no. 18, pp. 5821–5828, 2003.

[4] C. Hawthorne and I. Piper, "Monitoring of intracranial pressure in patients with traumatic brain injury," *Frontiers in Neurology*, vol. 5, article 121, 16 pages, 2014.

[5] T. S. Deisboeck and C. Guiot, "Surgical impact on brain tumor invasion: a physical perspective," *Annals of Surgical Innovation and Research*, vol. 2, article 1, 4 pages, 2008.

[6] E. Münch, P. Horn, L. Schürer, A. Piepgras, T. Paul, and P. Schmiedek, "Management of severe traumatic brain injury by decompressive craniectomy," *Neurosurgery*, vol. 47, no. 2, pp. 315–323, 2000.

[7] D. J. Cooper, J. V. Rosenfeld, L. Murray et al., "Decompressive craniectomy in diffuse traumatic brain injury," *The New England Journal of Medicine*, vol. 364, no. 16, pp. 1493–1502, 2011.

[8] C. P. Gao and B. T. Ang, "Biomechanical modeling of decompressive craniectomy in traumatic brain injury," *Acta Neurochirurgica, Supplementum*, vol. 102, pp. 279–282, 2008.

[9] J. A. Moore, Y. Li, D. T. O'Connor, W. Stroberg, and W. K. Liu, "Advancements in multiresolution analysis," *International Journal for Numerical Methods in Engineering*, vol. 102, no. 3-4, pp. 784–807, 2015.

[10] M. S. Greene, Y. Li, W. Chen, and W. K. Liu, "The archetype-genome exemplar in molecular dynamics and continuum mechanics," *Computational Mechanics*, vol. 53, no. 4, pp. 687–737, 2014.

[11] A. Goriely, S. Budday, and E. Kuhl, "Chapter two-neuromechanics: from neurons to brain," in *Advances in Applied Mechanics*, vol. 48, pp. 79–139, 2015.

[12] S. Budday, P. Steinmann, and E. Kuhl, "Secondary instabilities modulate cortical complexity in the mammalian brain," *Philosophical Magazine*, vol. 95, no. 28–30, pp. 3244–3256, 2015.

[13] A. Goriely, M. G. D. Geers, G. A. Holzapfel et al., "Mechanics of the brain: perspectives, challenges, and opportunities," *Biomechanics and Modeling in Mechanobiology*, vol. 14, no. 5, pp. 931–965, 2015.

[14] S. Budday, P. Steinmann, and E. Kuhl, "Physical biology of human brain development," *Frontiers in Cellular Neuroscience*, vol. 9, article 257, 2015.

[15] S. Budday, R. Nay, R. de Rooij et al., "Mechanical properties of gray and white matter brain tissue by indentation," *Journal of the Mechanical Behavior of Biomedical Materials*, vol. 46, pp. 318–330, 2015.

[16] A. Mohamed and C. Davatzikos, "Finite element modeling of brain tumor mass-effect from 3D medical images," in *Medical Image Computing and Computer-Assisted Intervention—MICCAI 2005: 8th International Conference, Palm Springs, CA, USA, October 26–29, 2005, Proceedings, Part I*, vol. 3749 of *Lecture Notes in Computer Science*, pp. 400–408, 2005.

[17] H. Kim, D.-H. Park, S. Yi et al., "Finite element analysis for normal pressure hydrocephalus: the effects of the integration of sulci," *Medical Image Analysis*, vol. 24, no. 1, pp. 235–244, 2015.

[18] S. Budday, C. Raybaud, and E. Kuhl, "A mechanical model predicts morphological abnormalities in the developing human brain," *Scientific Reports*, vol. 4, article 5644, 2014.

[19] S. Budday, P. Steinmann, and E. Kuhl, "The role of mechanics during brain development," *Journal of the Mechanics and Physics of Solids*, vol. 72, pp. 75–92, 2014.

[20] M. J. Razavi and X. Wang, "Morphological patterns of a growing biological tube in a confined environment with contacting boundary," *RSC Advances*, vol. 5, no. 10, pp. 7440–7449, 2015.

[21] M. Jalil Razavi, T. Zhang, T. Liu, and X. Wang, "Cortical folding pattern and its consistency induced by biological growth," *Scientific Reports*, vol. 5, article 14477, 2015.

[22] S. Budday, P. Steinmann, A. Goriely, and E. Kuhl, "Size and curvature regulate pattern selection in the mammalian brain," *Extreme Mechanics Letters*, vol. 4, pp. 193–198, 2015.

[23] S. Tang, Y. Li, W. K. Liu, and X. X. Huang, "Surface ripples of polymeric nanofibers under tension: the crucial role of Poisson's ratio," *Macromolecules*, vol. 47, no. 18, pp. 6503–6514, 2014.

[24] S. Tang, Y. Li, W. Kam Liu, N. Hu, X. He Peng, and Z. Guo, "Tensile stress-driven surface wrinkles on cylindrical core-shell soft solids," *Journal of Applied Mechanics*, vol. 82, no. 12, Article ID 121002, 2015.

[25] S. Tang, Y. Li, Y. Yang, and Z. Guo, "The effect of mechanical-driven volumetric change on instability patterns of bilayered soft solids," *Soft Matter*, vol. 11, no. 40, pp. 7911–7919, 2015.

[26] J. Yin, Z. Cao, C. Li, I. Sheinman, and X. Chen, "Stress-driven buckling patterns in spheroidal core/shell structures," *Proceedings of the National Academy of Sciences of the United States of America*, vol. 105, no. 49, pp. 19132–19135, 2008.

[27] X. Chen and J. Yin, "Buckling patterns of thin films on curved compliant substrates with applications to morphogenesis and three-dimensional micro-fabrication," *Soft Matter*, vol. 6, no. 22, pp. 5667–5680, 2010.

[28] R. J. H. Cloots, H. M. T. Gervaise, J. A. W. Van Dommelen, and M. G. D. Geers, "Biomechanics of traumatic brain injury: influences of the morphologic heterogeneities of the cerebral cortex," *Annals of Biomedical Engineering*, vol. 36, no. 7, pp. 1203–1215, 2008.

[29] J. Ho and S. Kleiven, "Can sulci protect the brain from traumatic injury?" *Journal of Biomechanics*, vol. 42, pp. 2074–2080, 2008.

[30] W. Hong, X. Zhao, J. Zhou, and Z. Suo, "A theory of coupled diffusion and large deformation in polymeric gels," *Journal of the Mechanics and Physics of Solids*, vol. 56, no. 5, pp. 1779–1793, 2008.

[31] X. X. Zhang, T. F. Guo, and Y. W. Zhang, "Formation of gears through buckling multilayered film-hydrogel structures," *Thin Solid Films*, vol. 518, no. 21, pp. 6048–6051, 2010.

[32] W. Hong, X. Zhao, and Z. Suo, "Formation of creases on the surfaces of elastomers and gels," *Applied Physics Letters*, vol. 95, no. 11, Article ID 111901, 2009.

[33] J. Zhang, X. Zhao, Z. Suo, and H. Jiang, "A finite element method for transient analysis of concurrent large deformation and mass transport in gels," *Journal of Applied Physics*, vol. 105, Article ID 093522, 2009.

[34] W. H. Wong, T. F. Guo, Y. W. Zhang, and L. Cheng, "Humidity-driven bifurcation in a hydrogel-actuated nanostructure: a three-dimensional computational analysis," *International Journal of Solids and Structures*, vol. 47, no. 16, pp. 2034–2042, 2010.

[35] W. H. Wong, T. F. Guo, Y. W. Zhang, and L. Cheng, "Surface instability maps for soft materials," *Soft Matter*, vol. 6, no. 22, pp. 5743–5750, 2010.

[36] Hibbitt, Karlsson, and Sorensen, *ABAQUS/Standard User's Manual*, vol. 1, Hibbitt, Karlsson & Sorensen, 2001.

[37] N. Kitchener, S. Hashem, M. Wahba, M. Khalaf, Z. Bassem, and S. Mansoor, *Critical Care in Neurology*, Flying, 2012.